Tri-D 3-D Printed Rocket Technical Report

Students for the Exploration and Development of Space:

University of California San Diego Chapter

Prepared by:

Teddy Zhang, Hung Chun Yang

Abstract

In this document, the authors aim to present the design process of a 3-D printed rocket engine (Tri-D). After the successful static fire in October 2013, Tri-D has become the first successful 3-D printed rocket engine to be designed and tested by a university. The engine is 200mm in length, with a throat and nozzle diameter of 18.62 and 39.35 respectively. Cooling is implemented using two methods. Regenerative cooling is achieved through integrated axial cooling passages with fuel as coolant, while the outer diameter of the injector plate uses fuel to film cool the chamber walls. With Liquid Oxygen and RP-1 mixed at an O/F ratio of 2.56 at the main elements, the engine is predicted to generate 0.839 kN of thrust. The main elements were of an F-O-O-F pattern, with the bores in a straight line. In designing the engine especially with regards to the inner passages and upstream manifolding of bipropellants, 3-D printing has provided the freedom to create almost any geometry by obviating limits imposed by traditional manufacturing methods.

Contents

1 List of Figures

2 Introduction

There currently exists a large demand to put various small payloads into space, a majority of which are small satellites, abbreviated small-sats. As modern microprocessors become smaller, faster and more economical every year, the ability to shrink satellite technology into a package weighing below one kilogram (Picosats) becomes increasingly prevalent. Today, there are numerous organizations and research teams headed by universities, military, and other private entities who have developed small-sat technology but need an efficient method of delivering them to orbit.

The present solution involves the aforementioned small-sats hitching a ride “piggybacking” with large launch vehicles. Dependence on large launch vehicles creates challenges mainly in time and cost. Hosts of large payloads and the launch service providers typically decide on the optimal launch time frame, forcing the small-sat creators to acquiesce to their schedules. A small-sat creator would be at the mercy of said parties; the long waitlist of small-sat launches usually means the dimensions, weight, and other requirements of the small-sat need to be finalized one or even two years in advance to launching. Furthermore, large launch vehicles are indefinitely complex, which subjects them to technical issues that often cause delays.

Development of rocket engines has been historically expensive and naturally intangible to the general public. Fabrication of a rocket engine requires the use of top-grade materials, tight tolerances, and manufacturing tools, with the latter costing significantly more as designs becomes more complex. With 3-D printing technology, complications and cost associated with the latter two challenges are drastically reduced, since the only tooling needed is a 3-D printer, and printing tolerances are generally lower than traditional manufacturing techniques. 3-D printing allows the engine to be made with less money without compromising performance.

The Tri-D project takes advantage of this fact and the engine contains complex internal passages that would be difficult to manufacture otherwise. This document aims to detail the design approach and justifications of which Tri-D was created with, starting from the initial requirements. Throughout the report, the design freedom offered by 3-D printing will be apparent. We hope the success of this project will lower the barrier to entry for amateur enthusiasts and professional organizations alike in the ever evolving pursuit for higher efficient and more cost effective solutions to propulsion.

UCSD SEDS TRI-D ROCKET

Students for the Exploration and Development of Space: UC San Diego Chapter

AT A GLANCE:

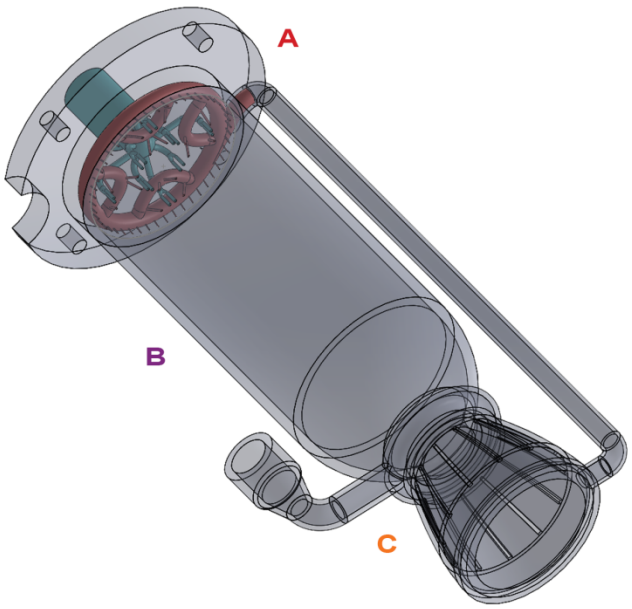

A THE INJECTOR PLATE

The FOOF Injector Plate, named after it's primary injector element pattern, has 8 symmetrically spaced elements, each consisting of dual of oxidizer orifices shooting vertically into the combustion chamber. They are impinged on the sides by a pair of fuel jets angled 40° inwards, hence arranging in a line a FOOF pattern. In addition, 48 fuel film cooling (FFC) holes streak the walls of the chamber spirally to cool the engine and concentrate the combustion towards the centerline.The FOOF Injector Plate takes advantage of 3-D Printing capabilities by ultilzing smooth circular passages greatly improving the efficiency of the flow.

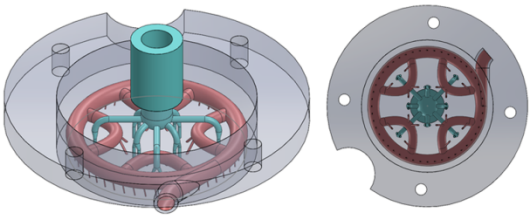

B THE ROCKET ENGINE

Given a starting design contraint of 100 lb thrust and and exit velocity of 3km/s, the design team set out to size the dimensions of the combustion chamber, throat, and nozzle. Using the Rocket Propulsion Analysis (RPA) program and confirming with hand calculations, the combustion chamber is roughly 2 in. in diameter by 5.5 in. in length. With a throat diameter of about .7 in. to the fully expanded nozzle diameter of 1.5 in., the entire rocket engine is roughly 8 inches in total length including the injector plate. The rocket engine is designed for a combustion pressure of nearly 300 psi at 1600° K.

C THE REGENERATIVE COOLING

The entire rocket engine was intended to be printed out as a single piece using the same material, Cobalt -Chromium. This would have virtually eliminated all manufacturing difficulties faced by conventional fabrication methods and makes including a regenerative cooling system as easy as adding a CAD model to the design. The TRI-D Rocket includes a simple regenerative cooling system that first feeds fresh RP-1 fuel to the temperature critical throat and then runs it through the nozzle, passing through heat sink vanes to maximize surface area cooling, and finally feeds into the injector plate.

SEDS

UC San Diego

Infograph Created by Hung Chun Yang

3 The Tri-D Rocket: A First Look

Figure 1: Tri-D Infographic

4 Design Requirements

The project initially started as a challenge from Jonathan E. Jones, a propulsion system engineer from NASA's Marshall Space Flight Center. Jones specified hypothetical initial conditions as shown below:

Thrust - *T = 444 N (100 lb)*

Delta V - *ΔV = 3 km/s*

Max Acceleration - a_{max} *= 5 g's*

The scope of this project was to explore a quick, cost-effective way to build small scale 3rd stage rocket engine. Since ΔV and max acceleration are parameters depend heavily on other aspects of a rocket, such as weight of components and throttling capabilities, this report will focus mainly on getting the thrust required with the engine. It should be noted that the thrust Tri-D aimed to achieve was *840 N* instead of the original value. After doing one iteration of design, it was found that an engine with *444 N* of thrust would simply have too small of an injector plate for the element pattern of choosing. The miniscule size of the injector plate would have prevented us from making intricate passages within, thus it was decided to proceed with double the thrust requirement.

5 Sizing

Sizing the thrust chamber, throat, and nozzle exits were the first step taken in the design process. Having the correct contraction and expansion ratios are imperative to achieving the desired exit velocity and thrust. The geometry was first calculated using theoretical thermodynamic equations. These equations will not be derived, as they are conveniently explained in almost all propulsion textbooks. After obtaining the results with hand calculations, Rocket Propulsion Analysis (RPA), a multi-platform software that predicts performance of rocket engines, is fed the same initial conditions. The outputs from RPA are then used for verification.

5.1 Assumptions

Thrust - T = 0.84 kN

Exit Pressure - P_{am} *= 1 atm = 101,325 Pa (ambient standard pressure)*

Oxidizer - Liquid Oxygen

Fuel - RP-1

Oxidizer/Fuel Ratio - O_F *= 2.56*

Molar Mass - M_m *= 22.1 kg/kmol*

Universal Gas Constant - R_u *= 8314.5 J/(K*kmol)*

Specific Heat Ratio - k *= 1.24*

Characteristic Length - L^* *= 1.0 m*

Chamber Temperature - T_0 *= 3670 K (RP-1 Combustion Temperature)*

Though Tri-D is the size of a 3rd stage rocket engine, it was designed to be static test fired on the ground. With that in mind, atmospheric pressure at sea level was taken to be the ambient pressure. The oxidizer and fuel were chosen to be liquid oxygen and RP-1, due to the high

efficiency associated with said combination. With the chosen propellants, modern textbooks and design guides generally recommend an O/F ratio of 2.4 – 2.6. A ratio of 2.56 was chosen because the specific heat ratio and combustion temperature assumed is generally accepted within the aerospace industry and attached to this mixture ratio (list source). Using previously established results by the industry grants the calculations much more credibility. The characteristic length for LOX and RP-1 has a recommended value of between 0.9 to 1.4 m (D. Huang p.72), and 1.0 was chosen as a starting point.

5.2 Preliminary Calculations

Calculations for sizing starts from Tsiokolvsky's rocket equation:

$$\Delta V = c \ln ln \left(\frac{m_0}{m_f} \right) \quad (1)$$

where m_0 is the wet mass of the rocket m_f is the final mass, or burnout mass of the rocket, and c is the effective exhaust velocity. In an ideal rocket, ΔV would be equal to c. Calculating through many iterations of thermodynamic relations, we concluded that an exit velocity of 3 km/s would be difficult to achieve. A more conservative exit velocity of 2.7 km/s was decided upon, for it is reasonable to assume 90% of an ideal rocket's efficiency. The total mass flow rate is given through the equation:

$$\dot{m} = \frac{T}{c} = 0.3 \text{ kg/s} \quad (2)$$

The average specific gas constant for the LOX/RP1 combination is given by:

$$R = \frac{R_u}{M_m} = 376.199 \text{ J/(kg K)} \quad (3)$$

Next, the exit velocity for a converging-diverging nozzle is given by:

$$c^2 = \left(1 - \frac{T_e}{T_0}\right) \frac{2kT_0R}{k-1} \quad (4)$$

where T_e is the exit temperature. Rearranging and solving for T_e/T_0 yields a ratio of *0.489*. Multiplying the ratio by T_0 leads to an exit temperature T_e of *1794.711 K*.

With the exit temperature calculated, the Mach number at the exit can now also be calculated:

$$M_e = \frac{c}{\sqrt{kRT_e}} = 2.951 \quad (5)$$

Ideal gas relations can be used to relate pressure to temperature:

$$\frac{P_e}{P_0} = \left(\frac{T_e}{T_0}\right)^{\frac{k}{k-1}} = 24.818E\text{-}3 \quad (6)$$

A perfect expansion of the nozzle would allow the exit pressure to be equal to that of the ambient pressure. With that in mind, P_e, the exit pressure, is set to be 1 atm. P_0, the chamber pressure, is then calculated to be *4.083 MPa*.

Equations for choked flow can be used to find the throat pressure and temperature:

$$T_t = \frac{T_0}{1+\frac{k-1}{2}} = 3276.786\ K \quad (7)$$

Using equation (6) again,

$$P_t = P_0\left(\frac{T_t}{T_0}\right)^{\frac{k}{k-1}} = 2.273\ MPa \quad (8)$$

The expansion ratio is defined as the ratio of nozzle exit area to throat area, which can be computed as follows:

$$\frac{A_e}{A_t} = \frac{1}{M_e}\left[\frac{2}{k+1}\left(1 + \frac{k-1}{2}M_e^2\right)\right]^{\frac{k+1}{2(k-1)}} = 5.627 \quad (9)$$

Assuming perfect gas law theory, the area of the throat can be found using the following equation,

$$A_t = \frac{\dot{m}}{P_t}\sqrt{\frac{RT_t}{k}} = 131.652\ mm\text{^}2 \quad (10)$$

Plugging A_t back into equation enables us to find A_e, which is *740.809 mm^2*. The diameters of the exit and throat, D_e and D_t respectively, can be found using the basic area of a circle equation. D_e and D_t are calculated to be *30.712 mm* and *12.947 mm* respectively.

The thrust coefficient is found using:

$$C_f = \frac{Thrust}{A_t P_0} = 1.563 \quad (11)$$

Using the assumed L^*, we calculated the chamber volume V_c using the equation:

$$V_c = L^* A_t = 131.652\ cm^3 \quad (12)$$

The length of the chamber is found using an empirically fitted formula:

$$L_c = EXP(0.029 \ln ln \left(D_t\right)^2 + 0.47 \ln ln \left(D_t\right) + 1.94) = 7.975\ cm \quad (13)$$ (include source)

Note that the above equation needs the throat diameters to be in units of cm, and the resulting answer is in cm as well.

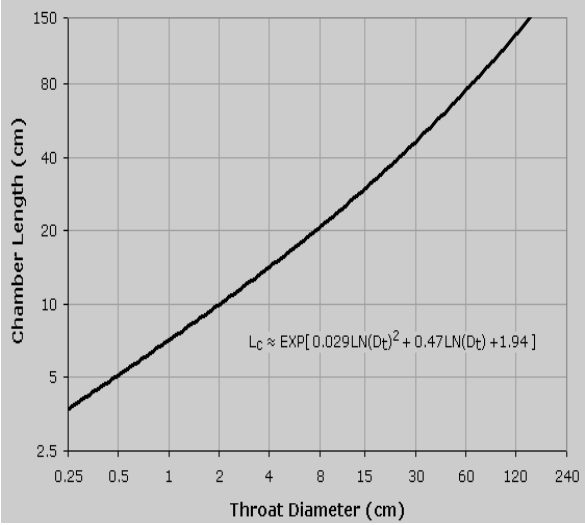

Figure 2: Empirical fitted formula for L_c

Next, an iterative method described by (source) is used to find a recommended chamber diameter:

$$D_c = \sqrt{\frac{D_t^3 + 24\tan tan\,(\theta)\, V_C}{D_c + 6tan(\theta) L_C}} = 66.091\ mm \quad (14)$$

where θ represents the half angle of the nozzle converging section, which is taken to be 15 degrees for preliminary calculations. The contraction ratio, defined as A_c/A_t is therefore calculated to be *26.058*. Next, the length of the nozzle, L_n, is calculated by using D_c, D_t, and θ to form a right triangle. L_n results in a value of *33.150 mm*.

5.3 RPA Results

As mentioned before, RPA was used to get concrete results and verify whether or not the above method of approach can be used reliably. To the extent possible, the same initial conditions and assumptions were used in RPA as in the above calculations. The inputs taken by the program were as follows: *L*, A_e/A_t, A_c/A_t, $\dot{m}$, P_c, $P_{ambient}$*, O/F ratio, and finally a choice of propellants. With the exception of P_c, A_e/A_t, and A_c/A_t, the other parameters were specified to the values used in the preliminary calculations.

Since a static test fire was planned with the Tri-D finished engine, there was a constraint of pressure achievable at the chamber. P_c was limited to 2 MPa; a mere 50% of the original calculated value. A lower chamber pressure meant the exit velocity would be lower, thus reducing the thrust. To counteract this effect, we chose to over-expand the nozzle, resulting in a lower P_e than the ambient pressure. Many iterations of RPA were executed by testing different expansion ratios until a good balance of exit pressure and thrust was achieved. Lastly, though the chamber diameter was calculated to be *66 mm*, the size proved to be excessive for our injector plate element pattern. Having found no credible recommendation against downsizing the chamber size coupled with the cost & weight savings associated with having a smaller D_c, it

was decided that a smaller contraction ratio was acceptable. The results of the final iteration of RPA are shown below:

```
SEDS April 29

Thrust and mass flow rates
-----------------------------------------
   Chamber thrust (vac):    0.83906     kN
 Specific impulse (vac):  285.20094      s
   Chamber thrust (opt):    0.73765     kN
 Specific impulse (opt):  250.73184      s
   Total mass flow rate:    0.30000   kg/s
Oxidizer mass flow rate:    0.21573   kg/s
    Fuel mass flow rate:    0.08427   kg/s

Geometry of thrust chamber with parabolic nozzle
-----------------------------------------
    Dc =   51.37  mm       b =   37.50 deg
    R2 =   33.36  mm      R1 =   13.62  mm
    L* = 1000.00  mm
    Lc =  140.95  mm    Lcyl =  103.37  mm
    Dt =   18.16  mm
    Rn =    3.47  mm      Tn =   14.82 deg
    Le =   40.90  mm      Te =   13.33 deg
    De =   39.35  mm
```

Figure X

```
# Engine name: SEDS April 29
# Mon Apr 29 20:52:58 2013
#
#*****************************************************************************************************************
# Propellant Specification
#-----------------------------------------------------------------------------------------------------------------
#    Component  Temp.          Mass           Mole
#                 [K]      fraction       fraction
#-----------------------------------------------------------------------------------------------------------------
#         RP-1  298.1     0.2808989      0.4721131
#        O2(L)   90.2     0.7191011      0.5278869
#-----------------------------------------------------------------------------------------------------------------
#              Total:     1.0000000      1.0000000
#-----------------------------------------------------------------------------------------------------------------
#    Exploded formula:  (O)1.056 (C)0.472 (H)0.921
#                O/F:     2.5600000
#             O/F 0:     3.4056663 (stoichiometric)
#             alpha:     0.7516885 (oxidizer excess coefficient)
#-----------------------------------------------------------------------------------------------------------------
#
# Table 1. Thermodynamic properties
#-----------------------------------------------------------------------------------------------------------------
#          Parameter       Injector      Nozzle inl      Nozzle thr      Nozzle exi             Unit
#-----------------------------------------------------------------------------------------------------------------
            Pressure         2.0000          1.9874          1.1544          0.0811              MPa
         Temperature      3487.4086       3485.9929       3323.9740       2618.5895                K
            Enthalpy      -788.4600       -792.4476      -1456.9218      -4183.4453            kJ/kg
             Entropy        11.7407         11.7419         11.7419         11.7419        kJ/(kg·K)
Specific heat (p=const)      7.5066          7.5091          7.2768          4.1878        kJ/(kg·K)
Specific heat (V=const)      6.3418          6.3442          6.2001          3.6525        kJ/(kg·K)
       Gas constant          0.3620          0.3619          0.3567          0.3364        kJ/(kg·K)
    Molecular weight        22.9705         22.9715         23.3085         24.7182
 Isentropic exponent         1.1310          1.1310          1.1275          1.1339
             Density         1.5844          1.5752          0.9736          0.0920            kg/m³
      Sonic velocity      1194.8776       1194.5863       1156.2583        999.3690              m/s
            Velocity         0.0000         89.3035       1156.2583       2605.7572              m/s
         Mach number         0.0000          0.0748          1.0000          2.6074
          Area ratio         8.0000          8.0000          1.0000          4.6945
           Mass flux       140.6666        140.6666       1125.7630        239.8037       kg/(m²·s)
            Viscosity         1.0821          1.0818          1.0479          0.8934      ·10?4 kg/(m·s)
Conductivity, frozen          0.3430          0.3428          0.3281          0.2636          W/(m·K)
Specific heat (p=const), frozen      2.0306          2.0305          2.0226          1.9743        kJ/(kg·K)
Prandtl number, frozen        0.6407          0.6407          0.6459          0.6692
Conductivity, effective       1.7093          1.7095          1.5920          0.7688          W/(m·K)
Specific heat (p=const), effective           7.5066          7.5091          7.2768          4.1878        kJ/(kg·K)
Prandtl number, effective             0.4752          0.4752          0.4790          0.4867
#-----------------------------------------------------------------------------------------------------------------
#
#-----------------------------------------------------------------------------------------------------------------
```

Figure X

```
# Table 2. Fractions of the combustion products
#-------------------------------------------------------------------------------------------------------------------------------------------------------
#          Species       Injector       Injector      Nozzle inl      Nozzle inl      Nozzle thr      Nozzle thr      Nozzle exi      Nozzle exi
#                     mass fract      mole fract      mass fract      mole fract      mass fract      mole fract      mass fract      mole fract
#-------------------------------------------------------------------------------------------------------------------------------------------------------
               CO      0.3948713       0.3238255       0.3948192       0.3237976       0.3827853       0.3185336       0.3300869       0.2912937
              CO2      0.2640578       0.1378233       0.2641399       0.1378725       0.2830645       0.1499179       0.3658863       0.2055025
             COOH      0.0000153       0.0000078       0.0000152       0.0000078       0.0000091       0.0000047       0.0000005       0.0000003
                H      0.0016743       0.0381571       0.0016741       0.0381533       0.0014538       0.0336187       0.0005439       0.0133389
               H2      0.0077378       0.0881699       0.0077371       0.0881670       0.0074694       0.0863642       0.0068461       0.0839453
              H2O      0.2431141       0.3099839       0.2431403       0.3100316       0.2514111       0.3252805       0.2812049       0.3858330
             H2O2      0.0000098       0.0000066       0.0000097       0.0000066       0.0000058       0.0000040       0.0000002       0.0000002
    HCHO,formaldehy      0.0000003       0.0000002       0.0000003       0.0000002       0.0000002       0.0000001       0.0000000       0.0000000
              HCO      0.0000154       0.0000122       0.0000154       0.0000122       0.0000087       0.0000070       0.0000004       0.0000004
             HCOOH      0.0000016       0.0000008       0.0000015       0.0000008       0.0000009       0.0000005       0.0000000       0.0000000
              HO2      0.0000880       0.0000612       0.0000876       0.0000610       0.0000542       0.0000383       0.0000019       0.0000014
                O      0.0107329       0.0154094       0.0107255       0.0153995       0.0082802       0.0120628       0.0009547       0.0014749
               O2      0.0290408       0.0208471       0.0290282       0.0208390       0.0242039       0.0176306       0.0035644       0.0027534
               OH      0.0486405       0.0656949       0.0486057       0.0656509       0.0412530       0.0565371       0.0109096       0.0158559
#-------------------------------------------------------------------------------------------------------------------------------------------------------
#
#-----------------------------------------------------------------------------------------------------------------
#
# Table 3. Theoretical (ideal) performance
#-----------------------------------------------------------------------------------------------------------------
#          Parameter      Sea level      Optimum ex          Vacuum            Unit
#-----------------------------------------------------------------------------------------------------------------
Characteristic velocity      0.0000       1771.0000          0.0000             m/s
Effective exhaust velocity       2521.2500       2605.7600       2943.7800             m/s
Specific impulse (by mass)       2521.2500       2605.7600       2943.7800           N·s/kg
Specific impulse (by weight)        257.1000        265.7100        300.1800                s
  Thrust coefficient          1.4236          1.4713          1.6622
#-----------------------------------------------------------------------------------------------------------------
#
#-----------------------------------------------------------------------------------------------------------------
#
# Table 4. Estimated delivered performance
#-----------------------------------------------------------------------------------------------------------------
#          Parameter      Sea level      Optimum ex          Vacuum            Unit
#-----------------------------------------------------------------------------------------------------------------
Characteristic velocity      0.0000       1721.6300          0.0000             m/s
Effective exhaust velocity       2374.3300       2458.8400       2796.8700             m/s
Specific impulse (by mass)       2374.3300       2458.8400       2796.8700           N·s/kg
Specific impulse (by weight)        242.1100        250.7300        285.2000                s
  Thrust coefficient          1.3791          1.4282          1.6245
#-----------------------------------------------------------------------------------------------------------------
#
#<b>Ambient condition for optimum expansion:</b>  H=1.84 km, p=0.800 atm
```

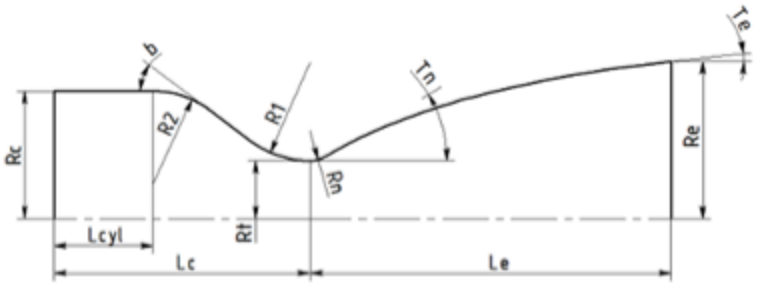

Figure 3: Nozzle Geometry References

As one might have predicted, the two sizing methods differed radically. Per the software program, an expansion ratio of only 4.695 would decrease the exit pressure to be 80% of standard sea level pressure. The C_f suggested by RPA is 1.6245 in vacuum compared with the previous value of 1.563. RPA produced a D_t 5 mm larger than was hand calculated, resulting in almost a 40% increase in radius and roughly 95% increase in area, though the latter effect may sound more detrimental than it actually is due to the sizes being small to begin with.

The differences in two methods may stem from a variety of reasons. Fundamental equations under the software are bound to differ from the first method; it is very likely that the software uses numerical methods to step through many calculations oversimplified by textbooks. Also very probably is the possibility that a lack of understanding of the theory may have led us astray in the preliminary calculations. Whatever the reason may be, the results generated by the software served as a foundation for the design. At the time of writing, it has yet to be proven that the software has yielded accurate, verifiable measurable results in the field.

6 Injector Element Pattern

6.1 Element Pattern

The element pattern chosen arranges four injectors lined up with the order of fuel-oxidizer-oxidizer-fuel (FOOF). This pattern is an improved version from the common triplet F-O-F and O-F-O designs. Below is a chart of the different element types considered along with their characteristics, listed from the order of perceived importance:

	F-O	F-O-F	O-F-O	O-F-F-O	F-O-O-F	F-O O-F	F-O F-O
Wall Compatibility	✔	✔	☐	☐	✔	✔	✔
Secondary Impingement	☐	☐	☐	✔	✔	✔	✔
Intrinsic Symmetry	☐	✔	✔	✔	✔	☐	☐
Momentum Distribution	☐	☐	✔	✔	✔	✔	☐
Proven Stability	✔	✔	✔	☐	☐	☐	☐

Wall compatibility is of the utmost importance due to the lack of regenerative wall cooling in the chamber and the likelihood of liquid oxygen disintegrating the wall material upon contact. Any pattern with oxygen being the outside element has the risk of LOX coming in contact directly with the wall. In fact, LOX elements that are shooting at a small angle incur the risk of missing the impingement point when pressurized and shooting directly into a wall.

With only a few element patterns being able to fit the scant space on the injector plate, it is imperative that each set of elements are able to fully atomize the propellants. Secondary impingement is created when a resultant stream from its first impingement point meets another resultant stream. The streams, in practice, are shaped more like cones, and unity of these two streams will ensure that any remaining propellants have a second chance at atomization. Patterns with four bores enjoy the option of secondary impingement, as the mixture from the first O-F pair can be directed at that of another O-F pair.

The next item of importance is intrinsic symmetry. Intrinsic symmetry is important because it allows the result vector to point directly down towards the throat by design. An O-F pair is asymmetric on a local level due to the 2.6 O/F ratio; unless the bore sizes are controlled very carefully and the injection speed is known indubitably, the resultant vector “cone” may not point axially. Following this logic, the last four element square pattern is ruled out, as it is simply two of these patterns combined. The alternating four element square pattern square does not have this characteristic either because the accuracy of the secondary impingement depends heavily on the primary impingements of the O-F pairs, bringing us back to the first concern. One can imagine that the four elements can simply meet at one point, but doing so would compromise the secondary impingement feature.

Momentum distribution is largely influenced by differences in bore size. An uneven spread of propellants and their momentum can potentially lead to large heat flux variations when combusted. However, the limited amount of element patterns and overall size of the engine minimizes the space available for significant heat fluxes to arise.

Lastly, each element pattern type has a certain degree of stability associated with it (insert that nasa source). The doublet and triplets have been extensively used and thus have proven their stability through many years of field experience. Similar to the previous point, we believe the size of the engine mitigates any effects of acoustic resonances and/or pressure fluctuations. Precautions are also taken by using high wall thicknesses to account for minor instability effects.

6.2 Injector Bores

The number of element patterns on the injector plate depends on the necessary mass flow rate required, and the pressure drop in the plate. The velocity of a fluid exiting out of an orifice is derived from Bernoulli's equation, which results in the following

$$V = C_d\sqrt{\frac{2\Delta P}{\rho}} \quad (15)$$

Multiplying both sides by ρ and A, the equation can be rearranged to

$$A = \frac{\dot{w}}{C_d\sqrt{2\rho\Delta P}} \quad (16)$$

where $\dot{w}$ is the propellant flow rate of a single orifice in kg/s. C_d is the orifice discharge coefficient, which is assumed to be the commonly accepted value of 0.7. ρ is density of propellant in kg/m^3; the density of LOX is assumed to be *1141 kg/m^3* and RP-1 *760 kg/m^3*. ΔP is the pressure drop across a system. Notice that in equation 15 shows that the velocity of the discharging fluid does not depend on area, but only on the pressure drop. The velocity coming out of a LOX hole of any size would be *18.665 m/s* and *24.250 m/s* for that of a fuel hole. In order for the propellant to flow out of the orifice consistently without backflow, ΔP is recommended to be at roughly 20% of the chamber pressure. As stated in section 5.3, the chamber pressure is limited to be 2 MPa, which produces a ΔP of *0.4MPa*. With the targeted O/F ratio of 2.56, the mass flow rate of RP-1 needs to be *0.0833 kg/s* and 0.*21667 kg/s* for LOX.

Using equation 16, it is found that a single RP-1 bore needs to have an area of 4.522 *mm^2* in order to achieve the desired mass flow. This area can then be divided by the number of bores desired on the injector plate to produce dimensions for each individual bore. However, 3-D printing is subjected to a minimum tolerance limit as in any other manufacturing technique. Direct Metal Laser Sintering (DMLS) suppliers generally wouldn't recommend any feature to have a diameter less than 0.3 mm. Since it was imperative that the main fuel holes emerge clean and unobstructed, we decided to limit a diameter of *0.6 mm* on the RP-1 bores, which

allows us to have 16 fuel bores on the injector plate. Using the same equations, it was found that with 16 LOX bores, the diameter on each hole would be *0.9 mm*.

For the film cooling (FC) holes on the outer boundary, different factors were taken into consideration. When designing injector plates for actual space applications, extreme caution is used in sizing FC holes to use the minimum cooling needed in order to save fuel weight and prevent ISP decline. Since the scope of this project is to prove feasibility in 3D printing applications, our priority was on making sure sufficient cooling was provided for the safety of the engine rather than minimizing fuel weight. In planning for the static fire test, it was desirable to have similar volumetric flow drain from both the RP-1 and LOX tanks, as to avoid either propellant running out before the other. This also allows the use of same size tanks and filling of each tank to the same volume, which facilitate testing setup by removing potential operation errors. In addition to cooling purposes, the FC holes served to regulate total flow rate of RP-1. More equivalent area provided by FC holes translates to more flow rate from the RP-1 tank. Unlike the main fuel bores in the primary elements, the FC bores were not limited in numbers by the geometry in upstream manifolding but rather by the minimum diameter printable by the supplier. However, more holes are desired to disperse an evenly distributed layer of fuel to the chamber walls. After several iterations it was decided that 32 cooling holes each with diameter of *0.37 mm* would be a conservative balance of fuel distribution, volumetric flow equivalence to LOX, and manufacturability. Finally, the resulting total volumetric flow rate from RP-1 tank and LOX tank are predicted to be 188.596 cm^3/s and 189.892 cm^3/s respectively.

6.3 Element Orientation and Geometry

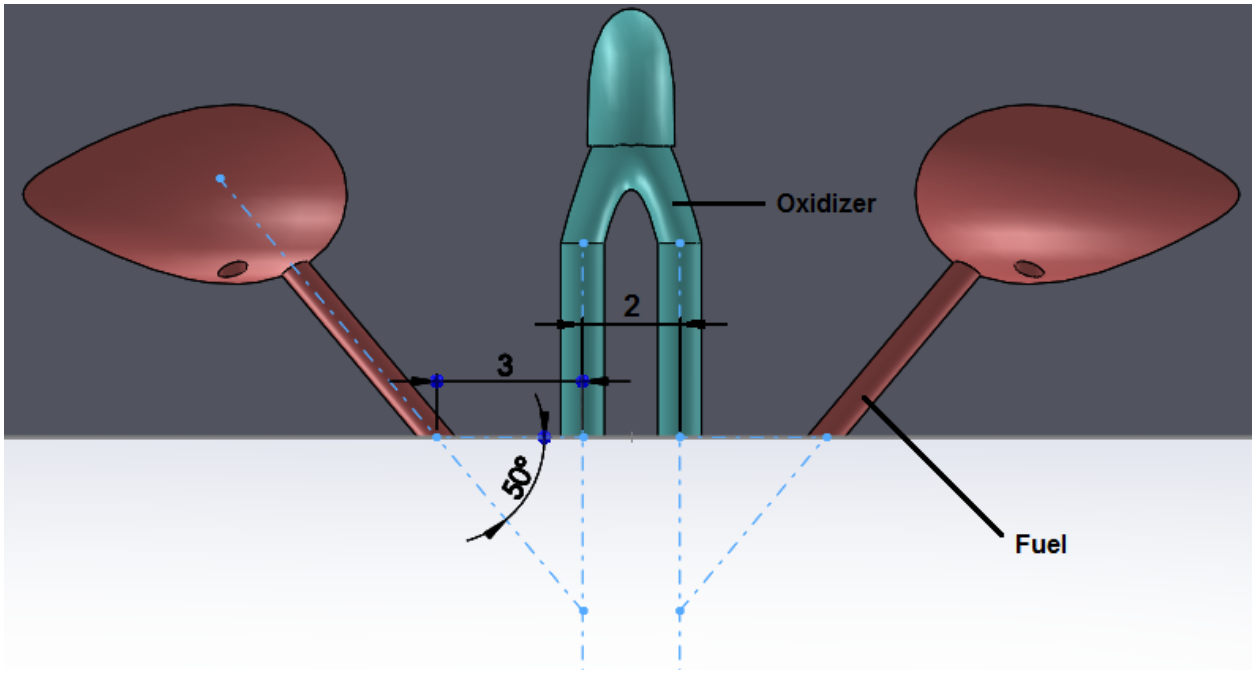

Figure 4: Close-up view of the FOOF element pattern

The F-O-O-F injector consists of an inner pair of oxidizer holes that point straight down and two fuel injectors which point 40 degrees with respect to the plate surface. The two center points of the oxidizer bore were placed 2 mm apart, and that of the oxidizer bore and the fuel bore were placed 3 mm apart. Our intent was to create primary impingement from the fuel and oxidizer that aims towards the center of the element pattern, which allows the resulting cones to merge and ensure total combustion of propellants. It is generally agreed that higher impingement angles result in better mixing and atomization. However, with impingement angles too high, one runs the risk of propellants back-splashing towards the injector plate, which can cause adverse heat flux on the plate itself and lead to premature failure of the engine. With a mere 40 degree impingement angle as opposed to the conventional 60-90 degrees, the risk of backsplash is considerably reduced. The trade-off here is poor mixing, thus secondary impingement becomes a crucial feature for combustion efficiency rather than a bonus feature. On a local level, placing the two oxidizers in the middle injecting straight down eliminates their radial velocity. In the case

of faulty impingement from RP-1, the fuel would shoot directly into the walls as opposed to the LOX shooting into the walls had they been placed at an angle. In addition, pointing the LOX straight down virtually eliminates any possibility of it back-splashing into the plate.

Using the 2-D equations for conservation of momentum and rudimentary vector geometry, the primary impingement point for each element is calculated to be at a distance of 3.575 mm from the injector plate, with a radial velocity of 4.330 m/s and axial velocity of 18.640 m/s. The secondary impingement point occurs at 7.880 mm from the injector plate, with only an axial velocity of 18.157m/s due to the two impinging cones being symmetric. In practice, velocities listed above would not be absolute due to the coning effect created by the impingement and simplicity of the equations used, and secondary impingement point is more of a gradual mixing, but these numbers serve as a quantitative metric when comparing different geometries through design iterations.

Lastly, each of the 32 film cooling holes on the outer boundary is pointed 10 degrees towards its clockwise adjacent neighbor. This configuration allows the film cooling larger surface coverage on the chamber walls, which also provides longer time for the film layer to cool the walls. Additionally, the swirling on the chamber walls would create vorticity in the combustion chamber, which we hypothesize would slightly decrease combustion efficiency by directing some energy radially in return for better ??

7 Injector Upstream Manifolding

Manifolding was done in a fashion that would reduce losses as much as possible and take advantage of 3D printing capabilities. Sharp corners and edges are rounded off wherever possible.

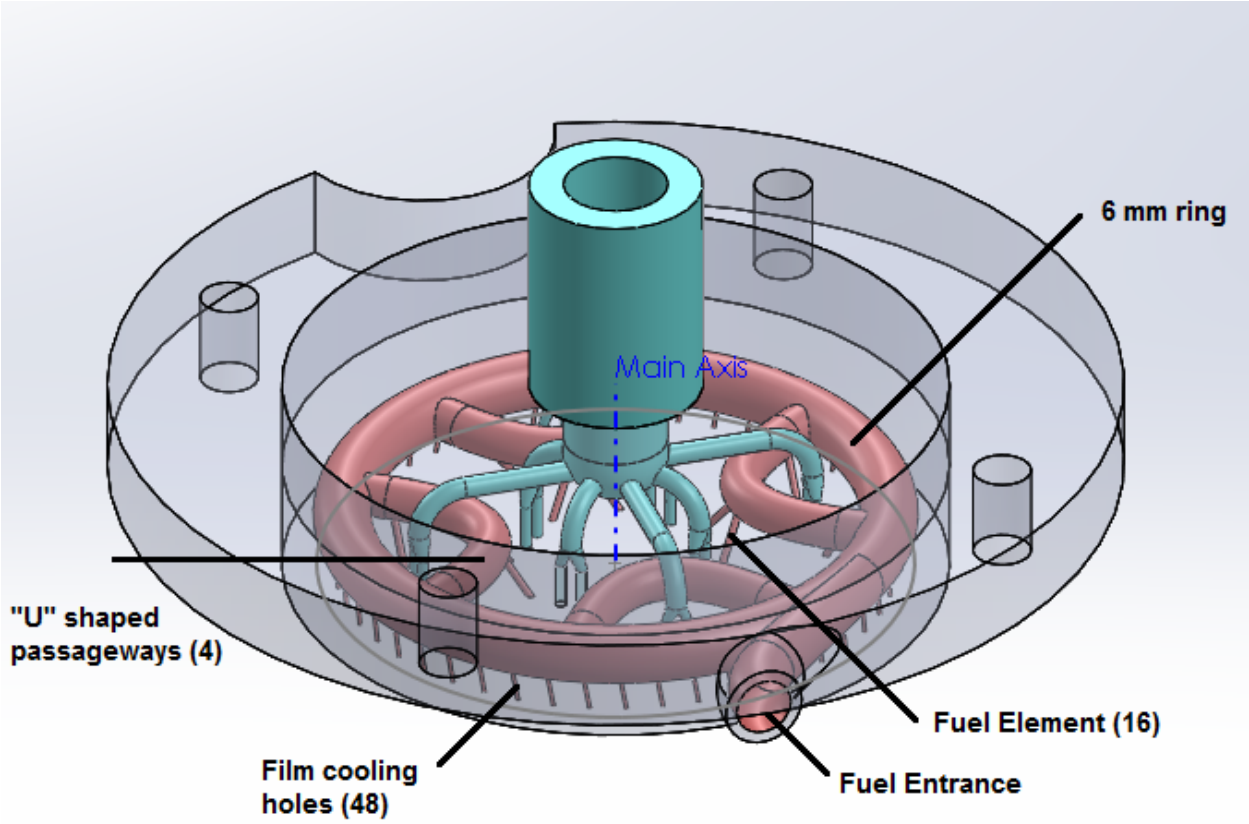

Figure 5: Close-up view of the fuel components

Fuel enters the injector plate into a 6 mm ring that encircles the perimeter from the side and at an angle to encourage a circular flow around the injector. This was done to reduce turbulent flow at the inlet, and attempt to keep equal pressure around the entire ring. All 48 film cooling holes stem from this ring. The 8 inner fuel elements are fed from 4 “U” shaped passageways that extrude from the ring. The outer elements are fed first, followed by the inner elements. It was found that feeding the outer elements first would have negligible effects on the pressure seen by the inner elements, and hence this design was selected as it also minimized total piping

found in the injector. Each of the outer elements have both fuel holes fed from an individual “U”, while the inner elements have one fuel fed from one “U” while the other fuel is fed from the neighboring “U”. This allows for the inner set of elements to be offset at 45 degrees from the outer set. Because each inner element is fed from two different “U” passageways, it is very important that each passage sees equal pressure. The large diameter used for the passages as well as the circular flow is designed to keep this the case.

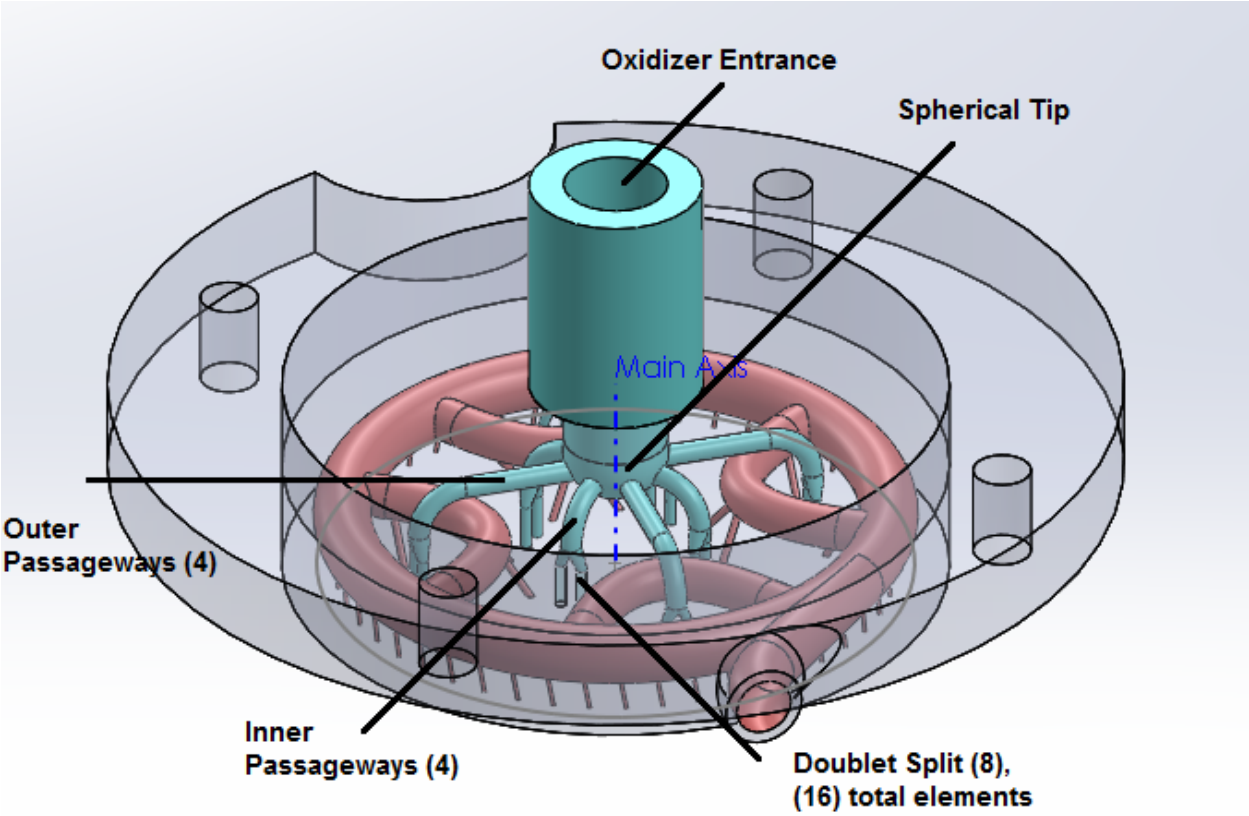

Figure 6: Close-up view of the oxidizer components

Oxidizer feeds straight down directly into the center of the injector plate. At the end of the oxidizer feeding pipe is a spherical tip, to minimize splashing of the liquid oxygen when the valves are first opened. From here, the cylindrical pipe splits off into 8 small passageways that feed directly to the oxidizer elements. All passageways come out at an equal height from the main oxidizer pipe to ensure equal pressure to all elements. Since each element actually requires two oxidizer holes, each of the 8 passageways splits into two smaller passageways

which then go straight down to the oxidizer element holes. This is done to minimize piping within the injector plate and retain the most structural integrity possible. When the passage splits into two, it is done in a smoothly curved manner to minimize turbulence so that flow comes out evenly from the oxidizers. Each passage for both fuel and oxidizer, before exiting to the combustion chamber, has at least a 4 mm straight section so fluid can exit in a settled manner.

8 Cooling

8.1 Assumptions

As previously made with the preliminary assumptions, These variables are taken from

adiabatic wall temperature T_{adi}= 3600 K

gas side wall temperature T_{gw}= 1600 K

diameter of the throat D_t= .01816 m

viscosity of gas μ_g= .8934*10^-4 kg/m-s

specific heat at constant pressure of gas c_{pg}= 1974.3 J/kg-K

Prandtl number of gas Pr_g=.669

Pressure of chamber P_c= 2*10^6 bar

Characteristic velocity c^*= 1771 m/s

Diameter of chamber D= 51.37mm

Chamber Temperature T_c=3600

Specific heat ratio γ=4.1878/3.6525

Mach number M=2.6074

Change in temperature of the wall sides ΔT= 420-1600K

Thermal conductivity k=11 W/m-K

8.2 Wall Thickness Calculation

Assuming a one dimensional steady state condition for the heat transfer from the throat of the engine and nozzle the combustion side convective heat flux can be found as follows

$$q_0 = h(T_{adi} - T_{gw}) \quad (17)$$

Where h, heat transfer coefficient of the gas side, can be found using Bartz correlation,

$$h = \left(\frac{.026}{D_t^{.2}}\right)\left(\frac{\mu_g^{.2} c_{pg}}{Pr_g^{.6}}\right)\left(\frac{P_c}{c^*}\right)\left(\frac{D_t}{D}\right)^{.18}\sigma \quad (18)$$

σ, correction factor for property variation across the boundary layer, can be found using the following equation

$$\sigma = \left[.5\left(\frac{T_{gw}}{T_c}\right)\left(1 + \frac{\gamma-1}{2}M^2\right) + .5\right]^{-.68}\left(1 + \frac{\gamma-1}{2}M^2\right)^{-.12} \quad (19)$$

Using the assumptions in section 7.1, σ is 1.09,and h is 2.123*10^6 W/m^2-K. Thus, q_0 is found to be.

Equating equation 17 to the conductive heat flux results in the following equation

$$q_0 = -k\frac{\Delta T}{\Delta x} \quad (20)$$

Using equation 20, Δx, thickness of the wall, is .003 mm.

8.3 Design

Before entering the injector plate, fuel travels first through a jacket around the nozzle of the engine. It enters at the throat into a 6 mm diameter ring circumventing it. Because this is the hottest part of the engine and requires the most cooling, the relatively large volume ring is designed to circulate fuel around before leaving to cool the rest of the nozzle. The rest of the nozzle from the throat down features a jacket that allows a 1 mm thick layer of fuel to travel between it and the nozzle.

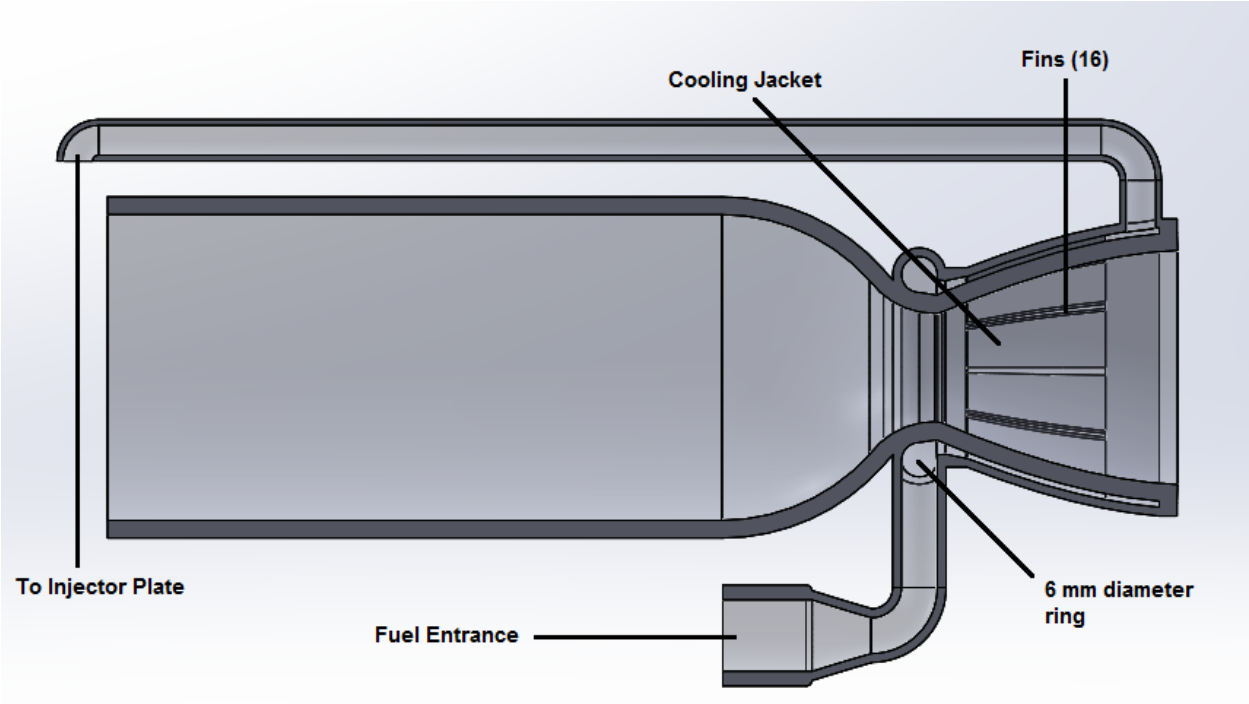

Figure 7: Close-up view of the thrust chamber

Within this thin layer, 12 “fins” protrude out connecting the nozzle and jacket. These are simply 0.7 mm thick dividers that serve as heat sinks by increasing surface area as well aiding in channeling fuel. Using the mass flow rate of fuel, .0833 kg/s, the velocity of the fuel traveling at both the throat section and the end of the nozzle can be found. At the throat the diameter is 18.05 mm, and at the nozzle exit the diameter is 32.03 mm, leading to approximate fuel velocities of 4.263 m/s and 2.230 m/s respectively.

9 The Static Test Fire

Stage 1: The vent/spill valves are opened, RP1 is relatively safe to handle so it is premeasured and filled from the top by the vent/spill valve, while LOX need to be handled more carefully so it is filled from the bottom through its fill valve. The vent/spill valves are normally closed, so they must be opened by pneumatic actuation of 150 PSI provided by the nitrogen tank.

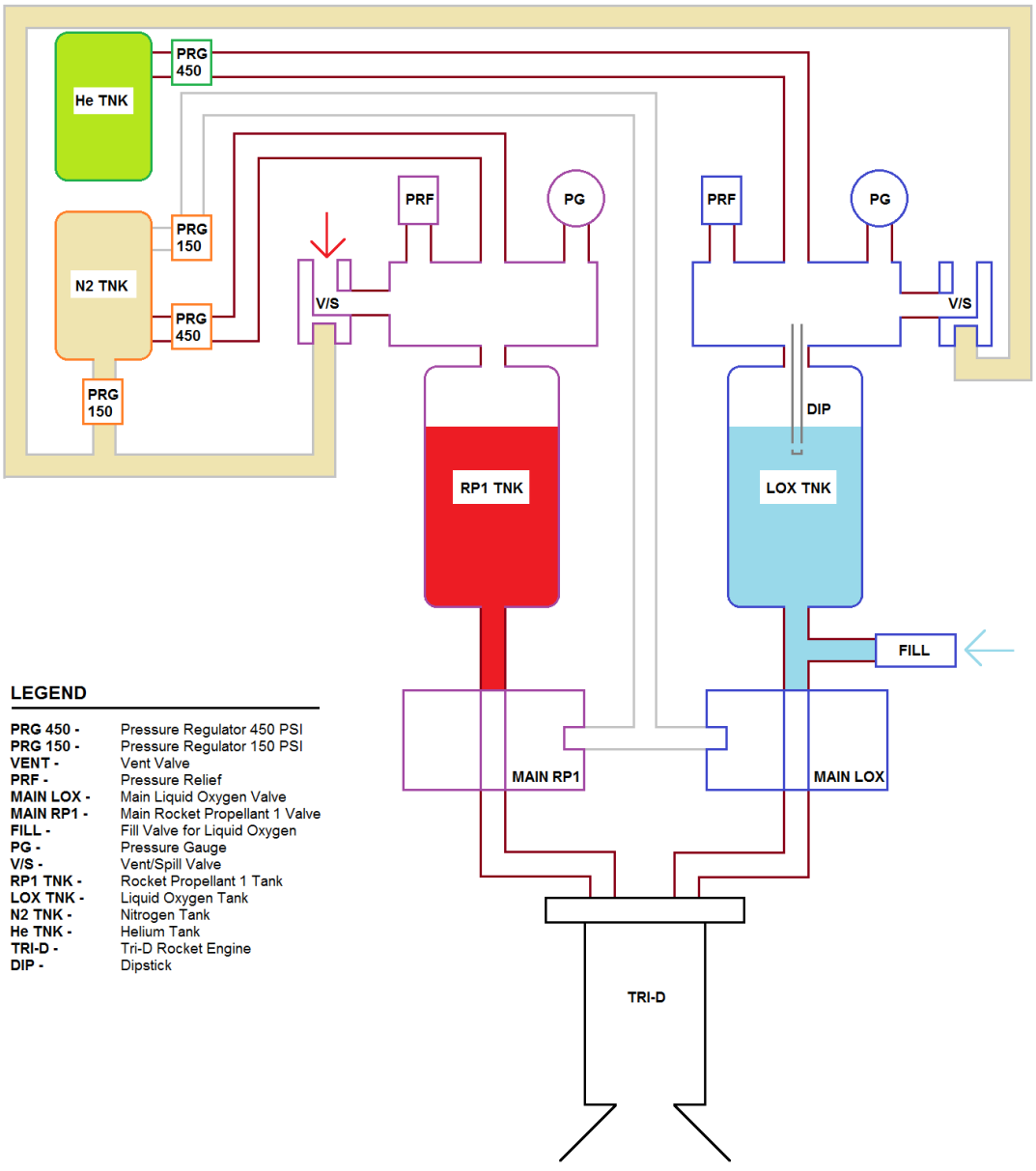

Figure 8: Static Fire Test Stage 1

Stage 2: Once filling is done, the vent/spill valves are closed by venting their pneumatic line. The system is then armed by turning on flow of the helium tank, as well as the main nitrogen line.

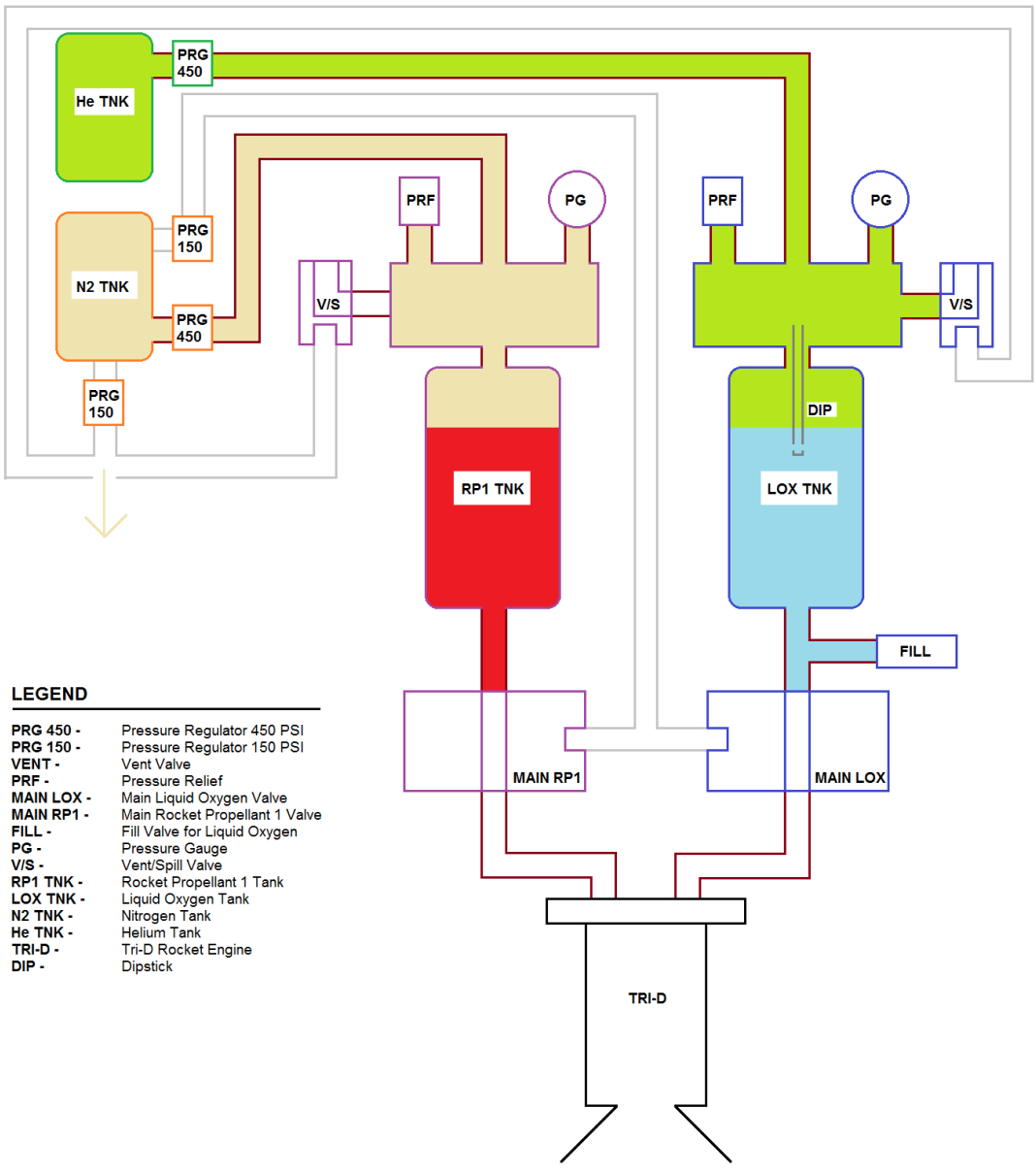

Figure 9: Static Fire Test Stage 2

Stage 3: The solid rocket igniter is electrically started and countdown is started. When countdown is reached, the final nitrogen pneumatic line is opened, and opens both main valves, starting the rocket engine.

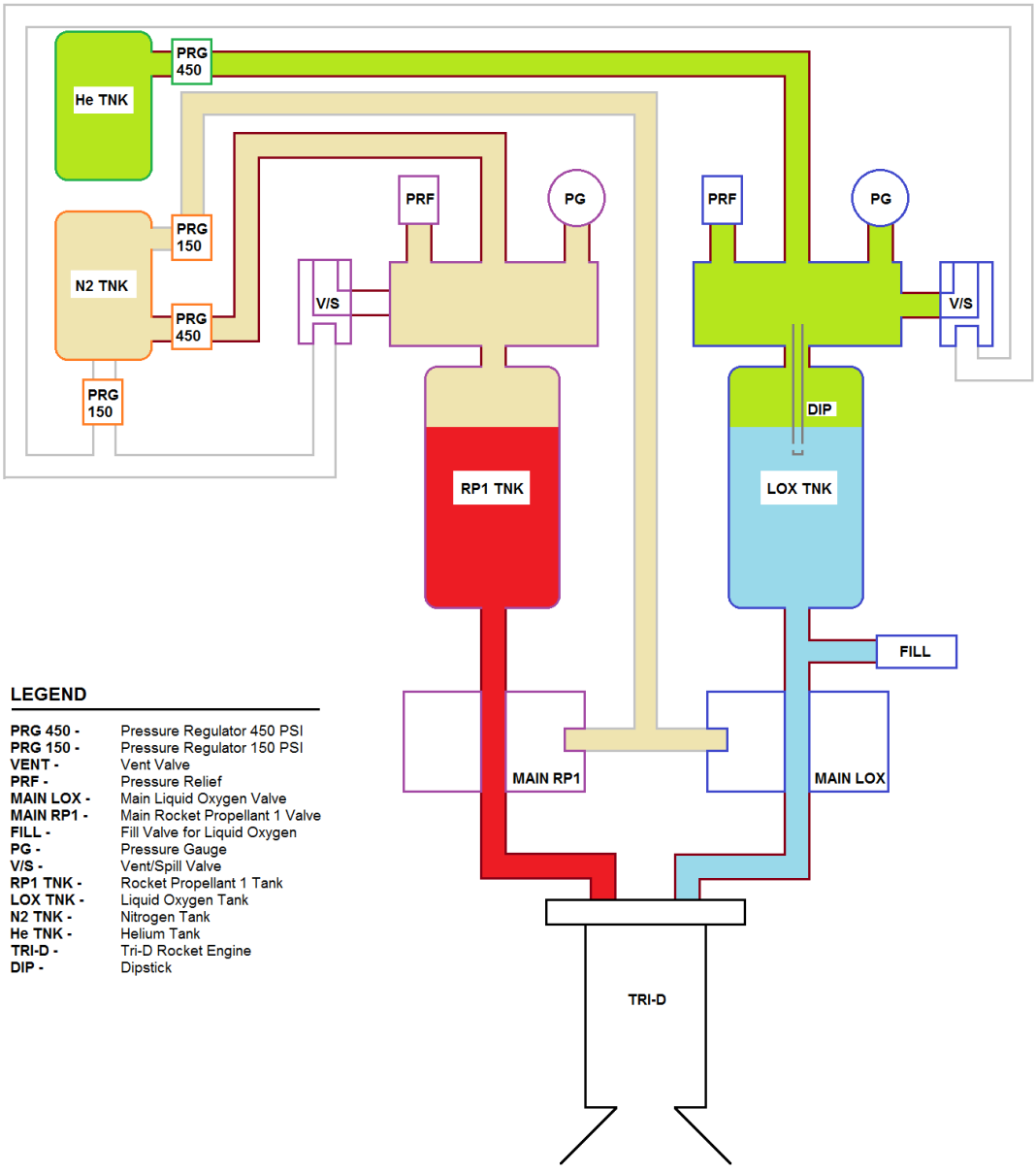

Figure 10: Static Fire Test Stage 3

Stage 4: When the desired burn time is reached, or an emergency situation requires an abort mission. The following steps are taken in order:

1. Helium and Nitrogen main lines are shutoff at the tanks.

2. Main valves are shut off by venting the nitrogen pneumatic line connected to the main valves

3. The vent/spill valves are opened and the pressure in the RP1 and LOX tanks is vented out.

The system is now disarmed and safe to approach.

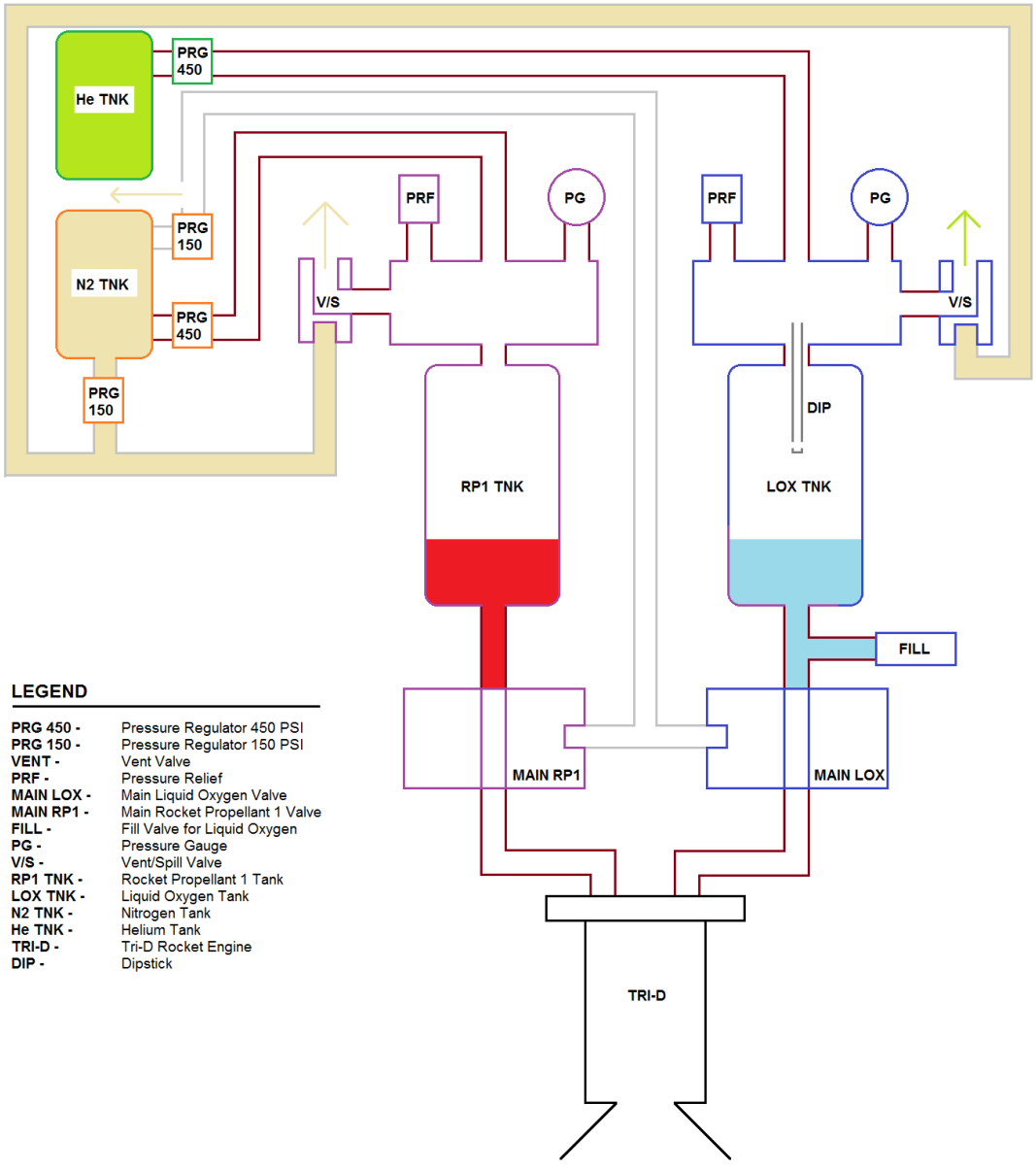

Figure 11: Static Fire Test Stage 4

10 Current Assessments

At the time of this technical report, the rocket engine has been printed out in two pieces (injector plate and thrust chamber) using DMLS (Direct Metal Laser Sintering) 3-D printer, with cobalt-chromium as the material of choice. The printing service was done by GPI Prototype & Manufacturing Services, Inc. and cost approximately $6000. The reason the rocket engine needed to be printed in two pieces is due limitations of current 3-D printing technology. DMLS printing is done by laying down a thin layer of the chosen material in powder form, and using a high powered laser to melt it locally. This is done over many iterations, layer by layer until the entire part is printed out. This method poses two challenges to design. The main disadvantage is that when printing layer by later, material cannot suddenly appear in a new layer, meaning as the 3-D printing machine sees a new layer, all of the portions which need to be sintered must be attached to the previous layer of a portion that was sintered. This may be solved by reorienting the way the part is to be printed, switching from top to bottom or bottom to top but does not solve for every situation, such as when both orientations require the geometric configuration.

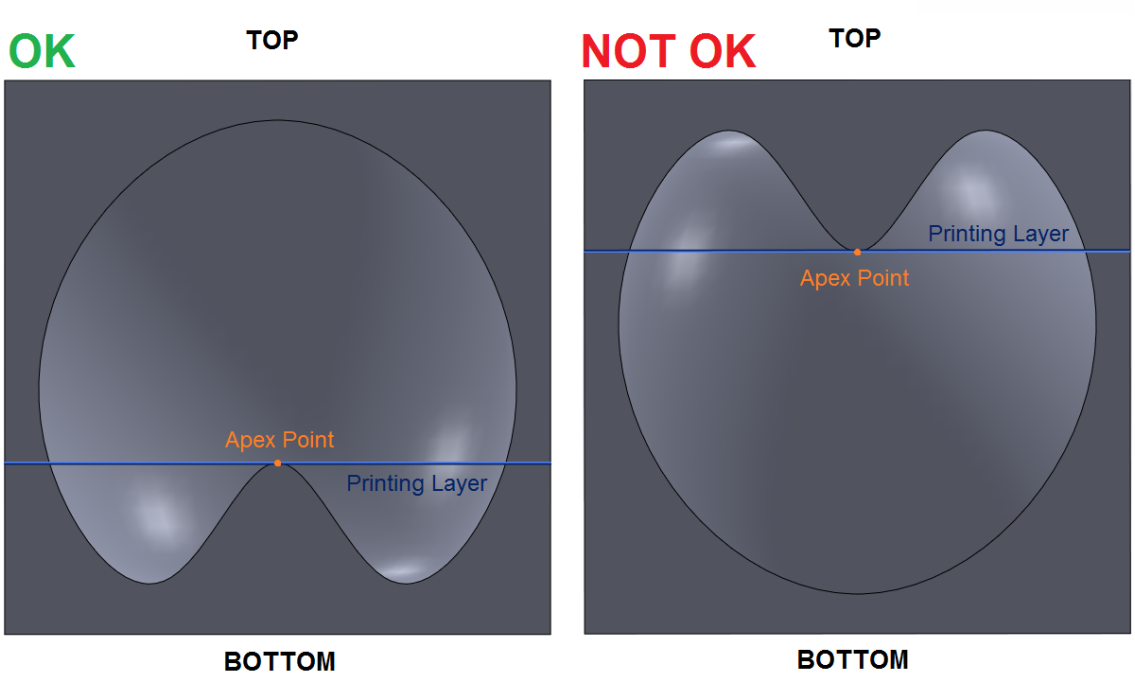

Figure 12: Example of a printable and unprintable component

Another limiting factor of 3-D printing is that it is not constrained by the amount of material or complexity of the part that needs to be printed, but rather the time it takes for a part to be printed is what determines the cost. There are currently a limited number of printers available for an abundant amount of customers who need their part printed. Therefore, this forces the price model to be based on the height of the part to be printed, as the time to print the part is directly correlated to how tall the part is. Rocket engines are traditionally long structures, and thus creates a problem of having a relatively high cost to print out. Initial quotes estimated the Tri-D rocket at $15000. Printing the rocket sideways is a possibility, but would need to fit within the printable area of the printer and may need supports to be printed additionally in order to stabilize the part while it is being printed. This would add additional manufacturing to the process as the supports would likely need to be removed after the part is finished.

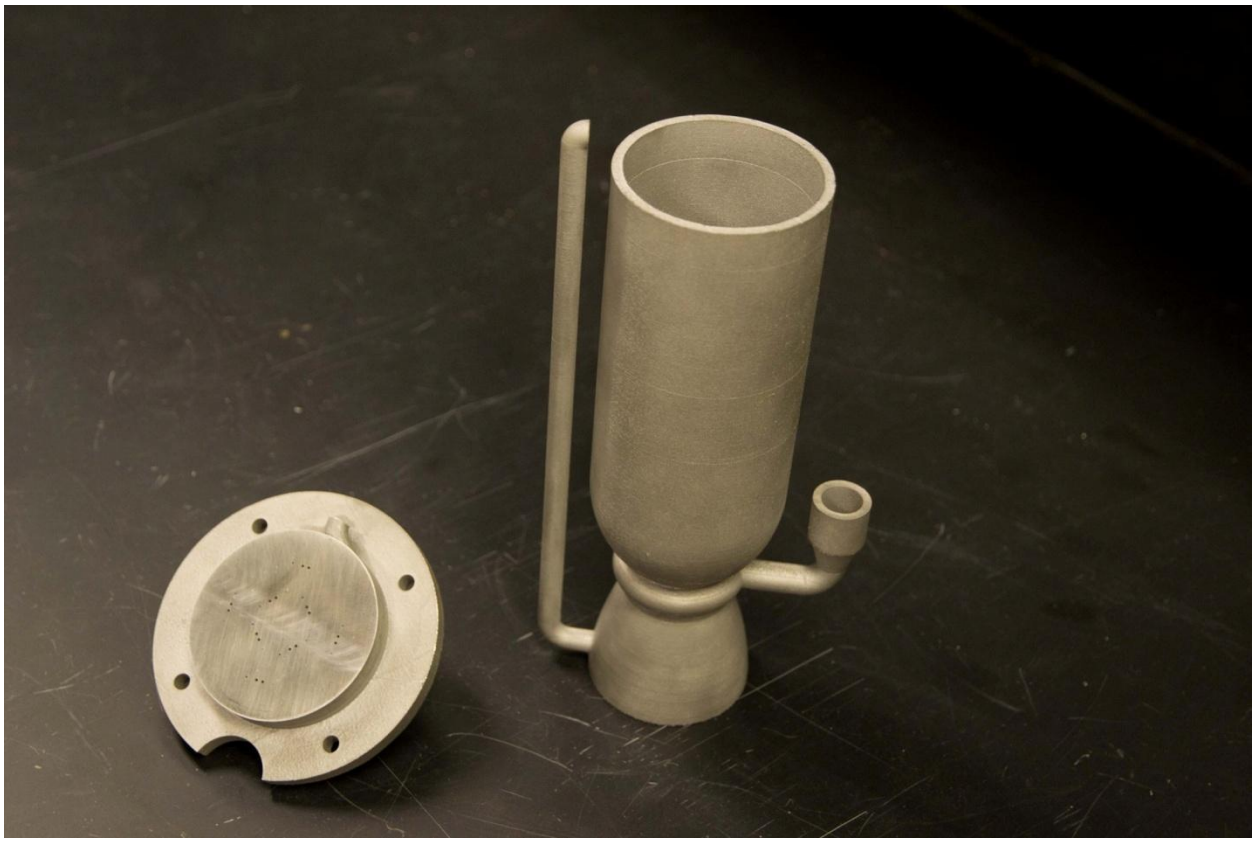

Figure 13: Photograph of the printed injector plate and thrust chamber

Though 3-D printing technology can be considered incredible in terms of how high of a resolution that can be printed, but it is not perfect. The UCSD SEDS team performed a water flow test on the printed injector plate and discovered that some of the film cooling holes were clogged during the printing process. These holes were .3 mm in diameter, and likely represents near the limit in resolution capabilities of current DMLS technology. This issue was solved by using wetted fine sandpaper to smooth the face of the injector plate. After this process, the clogged film cooling holes were opened. As seen in figure 9, only the injector face is smooth enough to be a reflective surface, while the rest of the surfaces, being untreated are relatively rough. From this ordeal, it can be stated that there is still room for improvement in the technology of DMLS in terms of precision and resolution capabilities for the use of 3-D printing miniature rockets.

11 Conclusions

Blah blah blah gene yang is super sexy and cool

12 References

http://www.braeunig.us/space/propuls.htm

yeah just put some bs references, most stuff is basically from this website ^^

13 Appendix

GENERAL LAYOUT

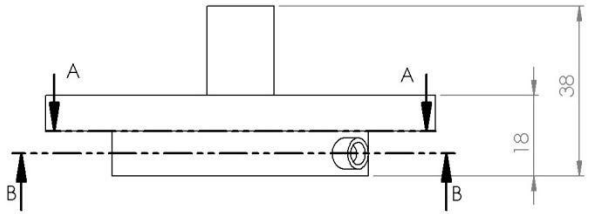

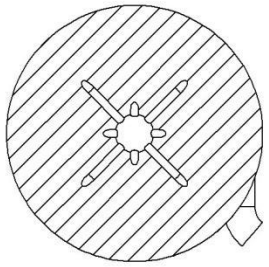

SECTION A-A

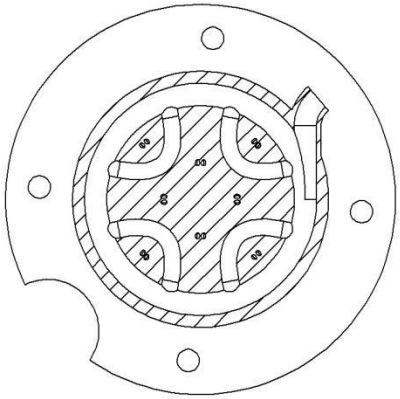

SECTION B-B

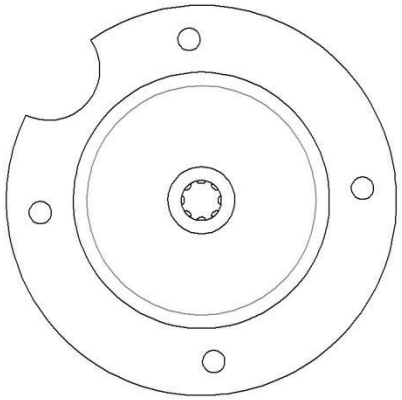

TOP VIEW

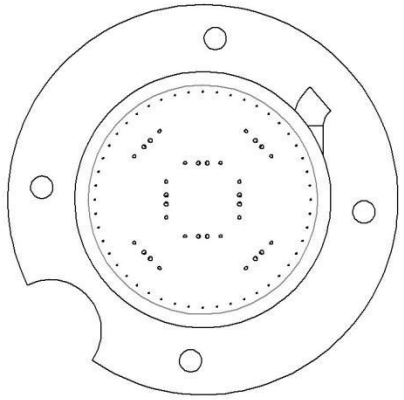

FACE VIEW

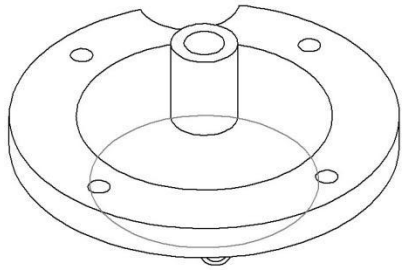

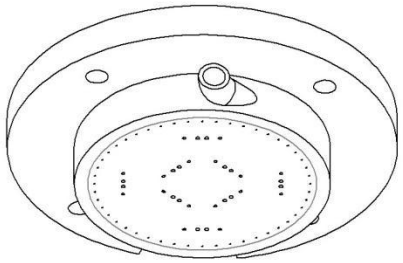

UNLESS OTHERWISE SPECIFIED: DIMENSIONS ARE IN MILLIMETERS SURFACE FINISH: TOLERANCES: LINEAR: ANGULAR:		FINISH:			DEBUR AND BREAK SHARP EDGES	DO NOT SCALE DRAWING	REVISION
	NAME	SIGNATURE	DATE			TITLE:	
DRAWN							
CHK'D							
APPV'D							
MFG							
Q.A				MATERIAL:		DWG NO.	A2
				WEIGHT:		SCALE:1:1	SHEET 1 OF 3

Tri-D Injector Plate v1.4

INJECTOR FACE DIMENSIONS

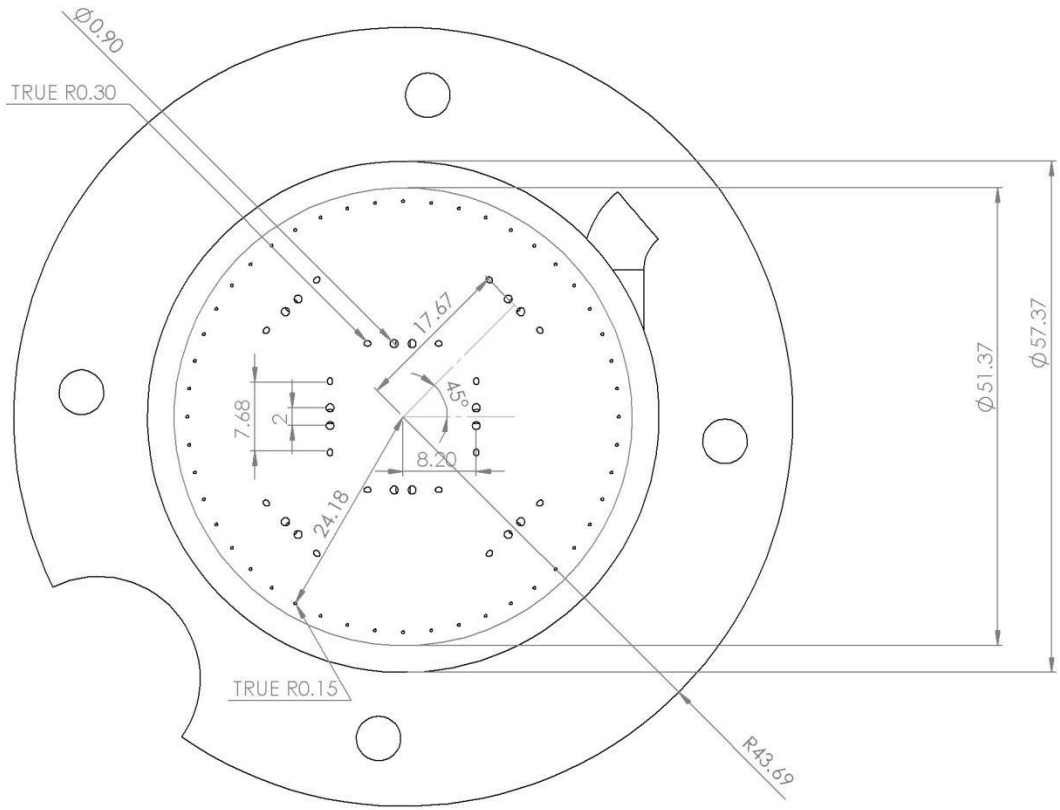

UNLESS OTHERWISE SPECIFIED: DIMENSIONS ARE IN MILLIMETERS SURFACE FINISH: TOLERANCES: LINEAR: ANGULAR:			FINISH:			DEBUR AND BREAK SHARP EDGES	DO NOT SCALE DRAWING / REVISION
	NAME	SIGNATURE	DATE				TITLE:
DRAWN							
CHK'D							
APPV'D							
MFG							
Q.A				MATERIAL:			DWG NO. A2
							Tri-D Injector Plate v1.4
				WEIGHT:			SCALE:1:1 / SHEET 2 OF 3

FUEL PASSAGE DIMENSIONS

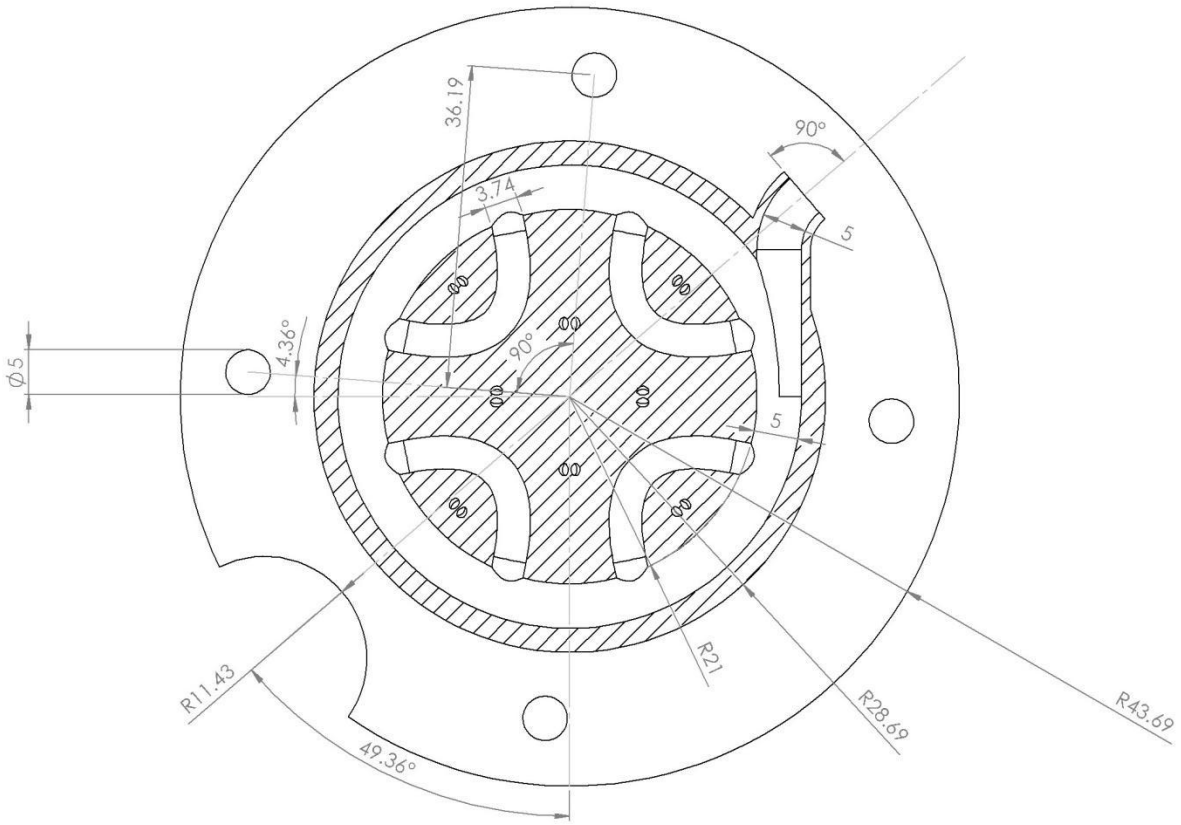

SECTION B-B
SCALE 2 : 1

UNLESS OTHERWISE SPECIFIED: DIMENSIONS ARE IN MILLIMETERS SURFACE FINISH: TOLERANCES: LINEAR: ANGULAR:		FINISH:				DEBUR AND BREAK SHARP EDGES	DO NOT SCALE DRAWING
	NAME	SIGNATURE	DATE				TITLE:
DRAWN							
CHK'D							
APPV'D							
MFG							
Q.A				MATERIAL:			DWG NO. Tri-D Injector Plate v1.4 A2
				WEIGHT:			SCALE:1:1 SHEET 3 OF 3

GENERAL LAYOUT

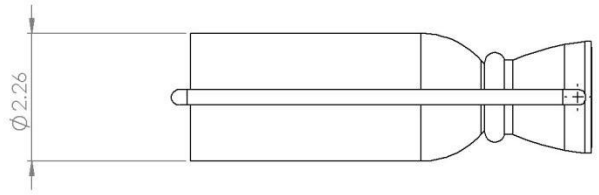

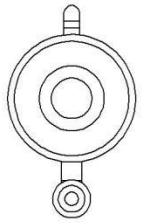

SECTION C-C

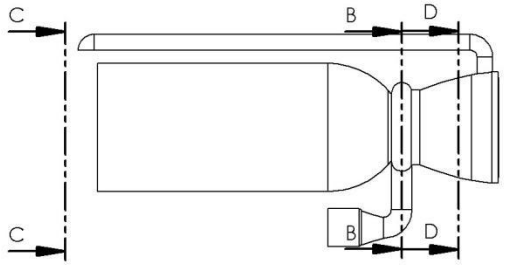

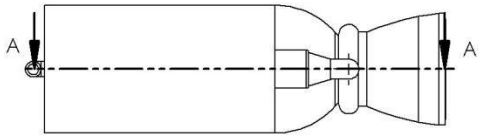

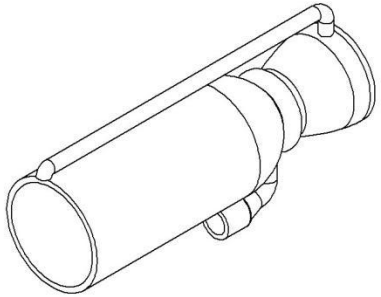

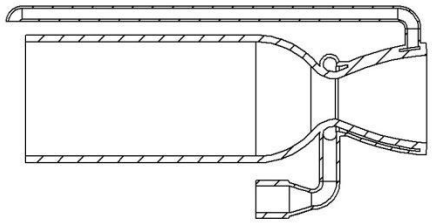

SECTION A-A

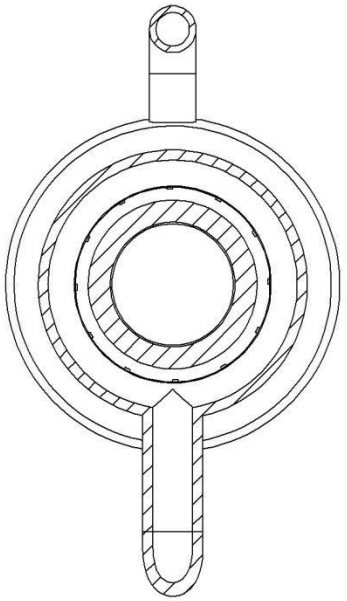

SECTION B-B
SCALE 1.5 : 1

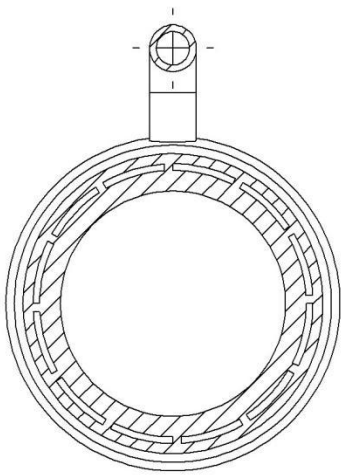

SECTION D-D
SCALE 1.5 : 1

UNLESS OTHERWISE SPECIFIED: DIMENSIONS ARE IN MILLIMETERS SURFACE FINISH: TOLERANCES: LINEAR: ANGULAR:			FINISH:			DEBUR AND BREAK SHARP EDGES	DO NOT SCALE DRAWING / REVISION
	NAME	SIGNATURE	DATE				TITLE:
DRAWN							
CHK'D							
APPV'D							
MFG							
Q.A				MATERIAL:			DWG NO. RegenCoolin 1.1 / A3
				WEIGHT:			SCALE:1:2 / SHEET 1 OF 2

Engine Chamber Nozzle & Regen Cooling

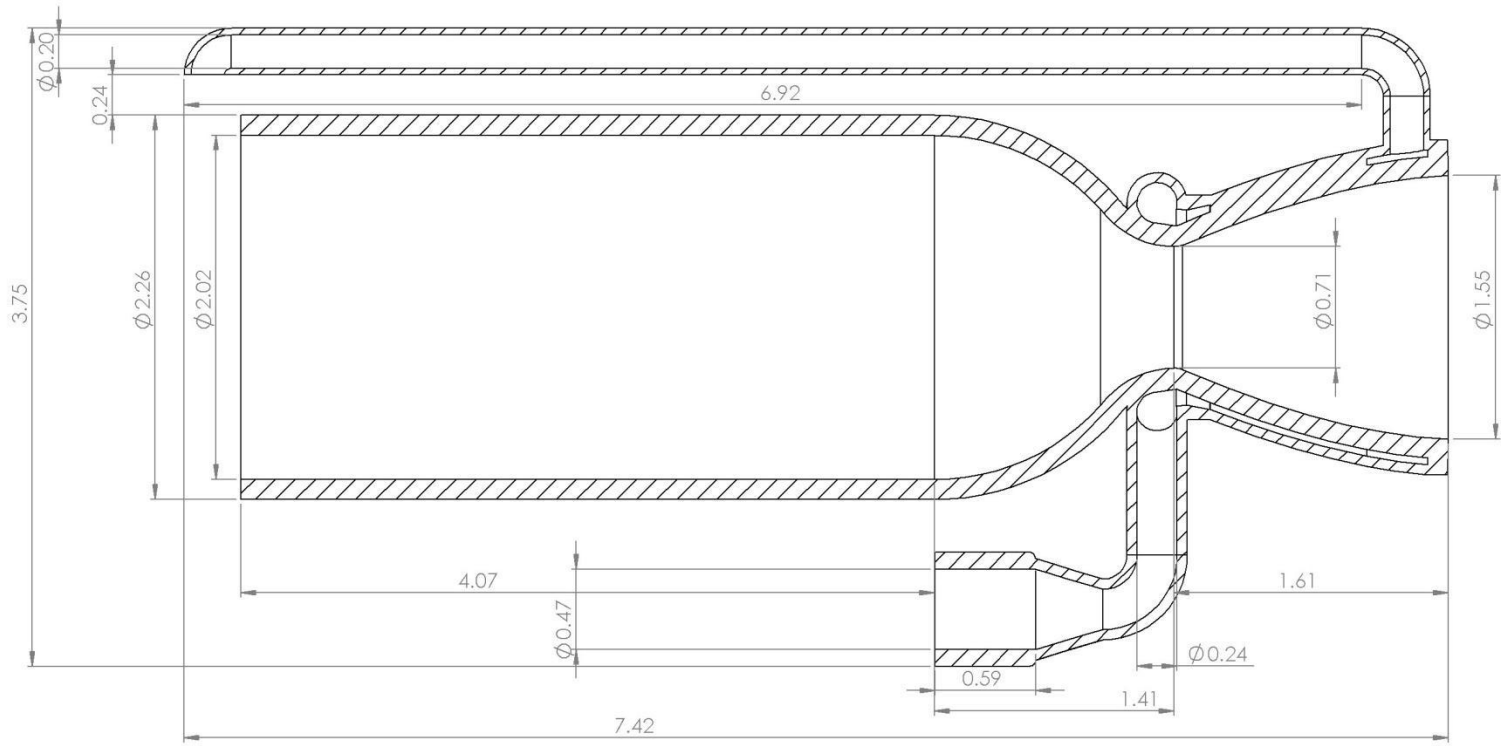

SECTION A-A
SCALE 1.5 : 1

UNLESS OTHERWISE SPECIFIED: DIMENSIONS ARE IN MILLIMETERS SURFACE FINISH: TOLERANCES: LINEAR: ANGULAR:		FINISH:			DEBUR AND BREAK SHARP EDGES	DO NOT SCALE DRAWING	REVISION
	NAME	SIGNATURE	DATE			TITLE:	
DRAWN							
CHK'D							
APPV'D							
MFG							
Q.A				MATERIAL:		DWG NO. RegenCoolin 1.1	A3
				WEIGHT:		SCALE:1:2	SHEET 2 OF 2